IEEE Access
Multidisciplinary | Rapid Review | Open Access Journal

Received 29 January 2023, accepted 17 February 2023, date of publication 22 February 2023, date of current version 3 March 2023.

Digital Object Identifier 10.1109/ACCESS.2023.3247821

RESEARCH ARTICLE

Broadband Dual-Polarized Magnetoelectric Dipole Antenna With Compact Structure for 5G Base Station

SHIHAO WU AND FENG SHANG
Provincial Key Laboratory of Electromagnetic Field and Microwave Technology, Xi'an University of Posts and Telecommunications, Xi'an 710121, China
Corresponding author: Feng Shang (476436868@qq.com)

ABSTRACT This paper presents a compact wideband dual-polarized magnetoelectric dipole antenna suitable for 5G base stations, which can cover 5G NR n77/78/79 band. The proposed antenna is configured with a cross ME dipole loaded with a rectangular slot, and two L-shaped feed lines are coplanar with the vertical patch, which makes the transverse size of the antenna more compact. The prototype size is 0.57 λ_{min} × 0.57 λ_{min} (length × width). According to the measured results, the operating band of the antenna is 3.06-5.28 GHz, and the impedance bandwidth is 53.2% of −10 dB. In the whole frequency range, the isolation between ports is less than −22 dB. Furthermore, metal baffles around the ground are used to stabilize the radiation pattern and improve the front-to-back ratio, achieving gains greater than 8dBi in the frequency band. However, the half power beam width (HPBW) exceeds 65°±5° for base station applications. The antenna has the advantages of broadband, high front-to-back ratio and low cross-polarization, and can be used as a good candidate antenna for 5G commercial small base stations.

INDEX TERMS Wideband antenna, magnetoelectric dipole antenna, dual-polarized antenna, compact structure, 5G base station applications.

I. INTRODUCTION

The fifth generation of mobile communication has begun to be commercialized. Sub-6GHz, as the mainstream frequency band of 5G, is widely deployed because of its advantages of high speed and low delay. Compared with 4G, the 5G NR N77 (3.3-4.2 GHz), N78 (3.3-3.8 GHz) and N79 (4.4-5 GHz) bands divided by 3GPP have higher operating frequencies and more dense spectrum [1]. This makes the miniaturization and wideband base station antenna become the future development trend.

Patch antennas and printed dipole antennas are two common types of base station antennas. In previous studies, patch antennas show the advantages of small size, low profile and easy integration, which is conducive to the miniaturization of base stations [2], [3], [4]. However, due to the narrow bandwidth of the original patch antenna, additional parasitic structures or air gap layers need to be loaded to expand the bandwidth, but the bandwidth is still not wide enough [5], [6]. Moreover, the feed network is often needed to realize the dual polarization, which increases the design complexity, and also introduces more transmission losses, resulting in the reduction of radiation efficiency. Printed cross dipole antennas are often directly supplied by coaxial cables or feed Balun, which can effectively improve the radiation performance. Several cross-dipoles with broadband and high-gain characteristics have been proposed [7], [8], [9], [10], [11], but they all have the disadvantage of having a large metal reflector and a high profile. In the design of reference [12], the dipole is embedded in the aluminum cube, which makes the overall structure of the antenna more compact and improves the impedance bandwidth and the isolation between ports, but the backward radiation is not well suppressed.

Inspired by the complementary antenna of Clavin et al., the magnetoelectric dipole antenna was first proposed by Professor Luk in 2006. The antenna is a combination of an electric dipole and a short-circuit patch, with stable radiation patterns and low backward radiation, while easily achieving

The associate editor coordinating the review of this manuscript and approving it for publication was Chinmoy Saha.

wide band characteristics. For example, in [13], [14], [15], [16], [17], [18], and [19], the ME antenna with high directivity and wide band characteristics is designed, but the above antennas are all single-polarized. In [20] and [21], the two pairs of magnetoelectric dipoles were placed orthogonal to realize double polarization, and the impedance matching at low frequencies was improved by loading metal rings and parasitic patches on the top, but the radiation pattern would be depressed or deformed at high frequencies. In reference [22], the use of defective metal walls ensures the stability of the radiation pattern and improves the gain at low elevation angles, but the bandwidth is narrow. Subsequently, a dual-polarized ME antenna suitable for 5G NR band was proposed in literature [23], [24]. In [23], the microstrip line aperture coupling feed was used to achieve broadband. However, this structure will result in a large amount of backward radiation, requiring high impedance surfaces to be loaded for rear lobe suppression, which increases design complexity and manufacturing costs.

The broadband dual-polarization ME antenna proposed in this paper can simultaneously meet the application requirements of 5G NR N77/78/79. The feeder and the vertical patch are coplanar, which makes the overall structure of the antenna more compact and is conducive to miniaturization. In addition, the antenna has high gain, high front-to-back ratio, stable radiation mode and low cross- polarization. It can effectively improve the channel capacity and transmission quality of the communication system, and help to reduce the construction cost and space of the base station.

II. ANTENNA CONFIGURATION

The structure of the proposed dual-polarized magnetoelectric dipole antenna is shown in Figure 1. It consists of two pairs of horizontal tapered patches, vertical patches with curved rectangular slots, two L-shaped feeders, and a square cavity. The vertical patch and the ground between them form a magnetic dipole, and the horizontal tapered patch acts as an electric dipole. By orthogonal placement, dual polarization is achieved.

In order to make the overall structure of the antenna more compact and ensure the effectiveness of feeding, four symmetrical rectangular slots are loaded on the basis of the original magnetoelectric dipole in the design. The L-shaped feeder is extended through the rectangular slots and is in the same plane with the vertical patch. Feed by connecting the probe of the SMA connector to the bottom of the feeder, the outer conductor is connected to the ground. All structures are made of sheet metal of a certain thickness, which can effectively reduce substrate loss. The proposed antenna has a compact structure with an overall size of 56mm×56mm×19.4mm. The simulation and parameter optimization are carried out by HFSS software. The detailed dimensions are given in Table 1.

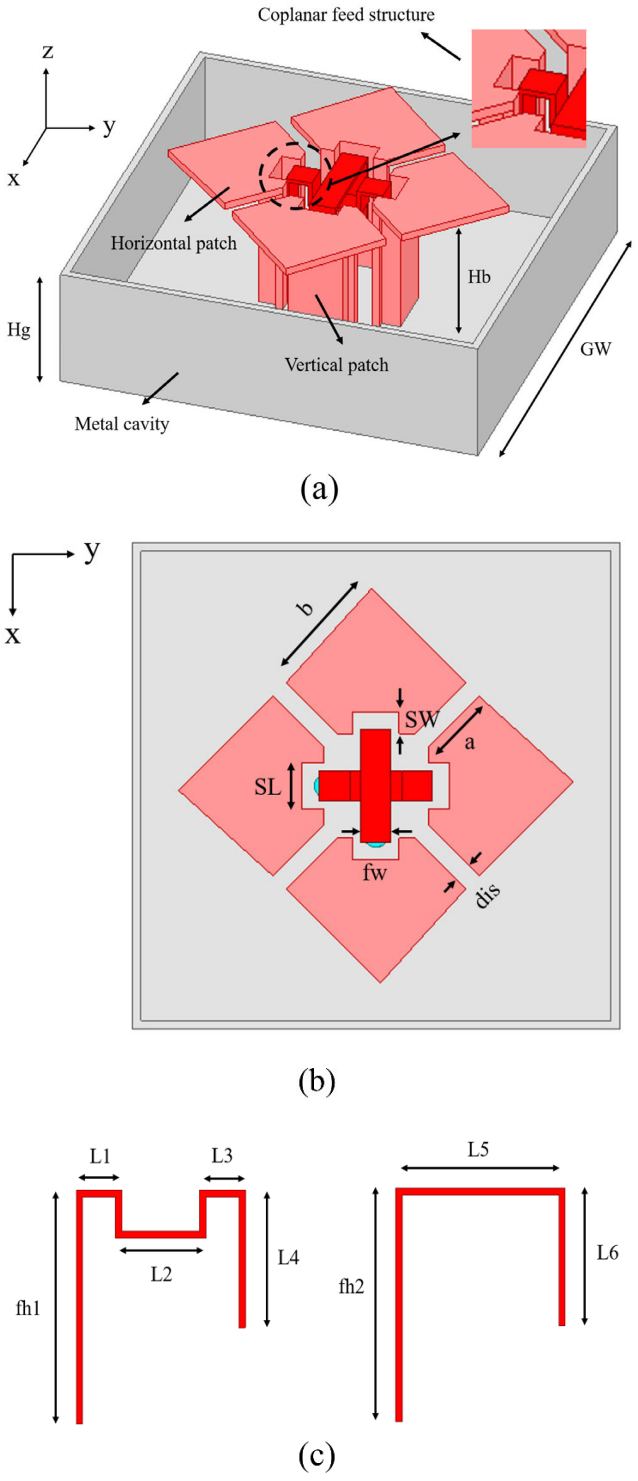

FIGURE 1. Diagram of the proposed ME antenna. (a) Overall view, (b) Top view, (c) Side view of two γ-shaped feeders.

III. BASIC THEORY AND WORKING PRINCIPLE

Magnetoelectric dipole antenna is proposed under the concept of complementary source. It consists of a basic electric dipole and a magnetic dipole. The electric dipole radiates in an 8-shape on the E-plane and an O-shape on the H-plane, while the magnetic dipole radiates in an O-shape on the E-plane and an 8-shape on the H-plane. As shown in the Figure 2, if the two dipoles are excited with the same

TABLE 1. Parameters of the proposed antenna.

Parameter	Value (mm)	Parameter	Value (mm)	Parameter	Value (mm)
Hb	17.4	*GW*	56	*Hg*	16
sw	2.5	*SL*	5.3	*dis*	2.2
fw	3.5	*a*	9.2	*b*	15.5
fh1	17	*L1*	3.5	*L2*	6
L3	3.5	*L4*	10	*fh2*	17
L5	13	*L6*	10		

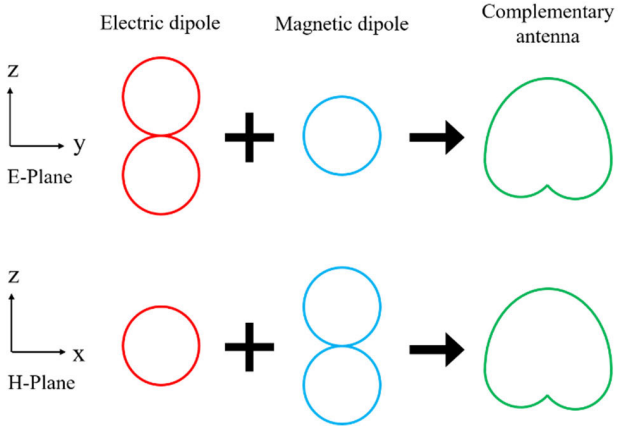

FIGURE 2. Schematic diagram of magnetoelectric complementarity in E-plane and H-plane.

amplitude and phase, their radiation patterns will be superimposed on each other, and the same heart-shaped pattern will be generated on the E plane and the H plane, so as to suppress the back radiation well.

Figure 3 depicts the equivalent circuit of the complementary antenna. The electric dipole and magnetic dipole operating in the basic mode can be approximately equivalent to the series resonant circuit represented by R_E, C_E, L_E and the parallel resonant circuit represented by R_M, C_M, L_M, respectively. Where R, L and C stand for resistance, inductance and capacitance in the circuit. When two resonant circuits are connected in parallel, the input admittance of the magnetoelectric dipole antenna can be expressed as follows:

$$Y_{in} \approx \left[\frac{1}{R_E} + \frac{1}{R_M}\right] - j\left[\left(\omega L_E - \frac{1}{\omega C_E}\right)\frac{1}{R_E^2} - \left(\omega C_M - \frac{1}{\omega L_M}\right)\right]$$

Here, the influence of capacitor C_f and inductor L_f caused by feeding is ignored. When the resonant frequency of the electric dipole is the same as that of the magnetic dipole, and the input resistance R_E of the electric dipole is adjusted to a value related to the reactance component, the imaginary part of the antenna cancels. The input admittance is only dependent on the resistance, which means that the broadband

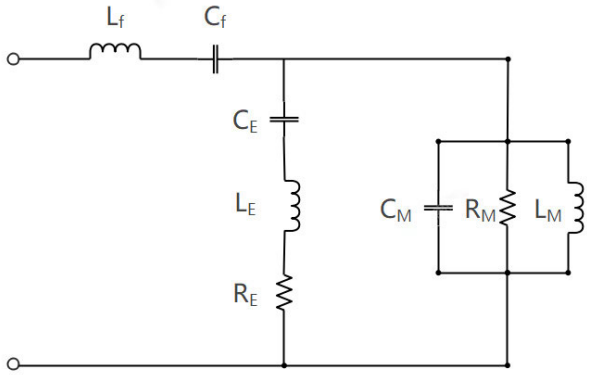

FIGURE 3. The equivalent circuit of a typical magnetoelectric dipole antenna.

characteristics can be achieved by choosing an appropriate antenna size.

In order to clearly illustrate the working mechanism of the antenna, Figure 4 plots the surface current distribution of the antenna under the excitation of two ports respectively, where T represents a period of time. When port 1 is excited, the current on the horizontal patch reaches its minimum value at t=0 (t=T/2). The strong current is mainly distributed along the vertical patch and is equivalent to the magnetic dipole in the x-axis direction. When t=T/4 (t=3T/4), the current intensity near the edge of the horizontal patch is dominant, while the current at both ends of the vertical patch is weak and has opposite paths, cancelling each other out, which is equivalent to the electric dipole in the y-axis direction. The antenna under port 2 excitation works similarly, while the amplitude of the current is equal, but the phase is opposite. This phenomenon shows that the current distribution of the antenna changes periodically, which proves that it works under the basic ME dipole mechanism.

IV. PARAMETER STUDY

A. EFFECT OF THE SW

Figure 5 shows the influence of the rectangular slot width sw on the reflection coefficient. While keeping other parameters unchanged, the impedance matching at low frequency is improved with the increase of sw, but the resonant frequency moves to higher frequency, which will narrow the operating bandwidth. At high frequencies, the resonant frequency is basically unaffected, but the impedance matching increases. Based on the simulation phenomenon, the antenna performance reaches the best when sw is 2.5 mm.

B. EFFECT OF THE FH1

The influence of feeder height fh1 on reflection coefficient is shown in Figure 6. With the increase of fh1, the high-frequency resonance of the antenna moves slightly to the right, and the impedance rises, but the change is not significant. The resonance and working bandwidth at the low frequency are almost not affected, and the impedance matching

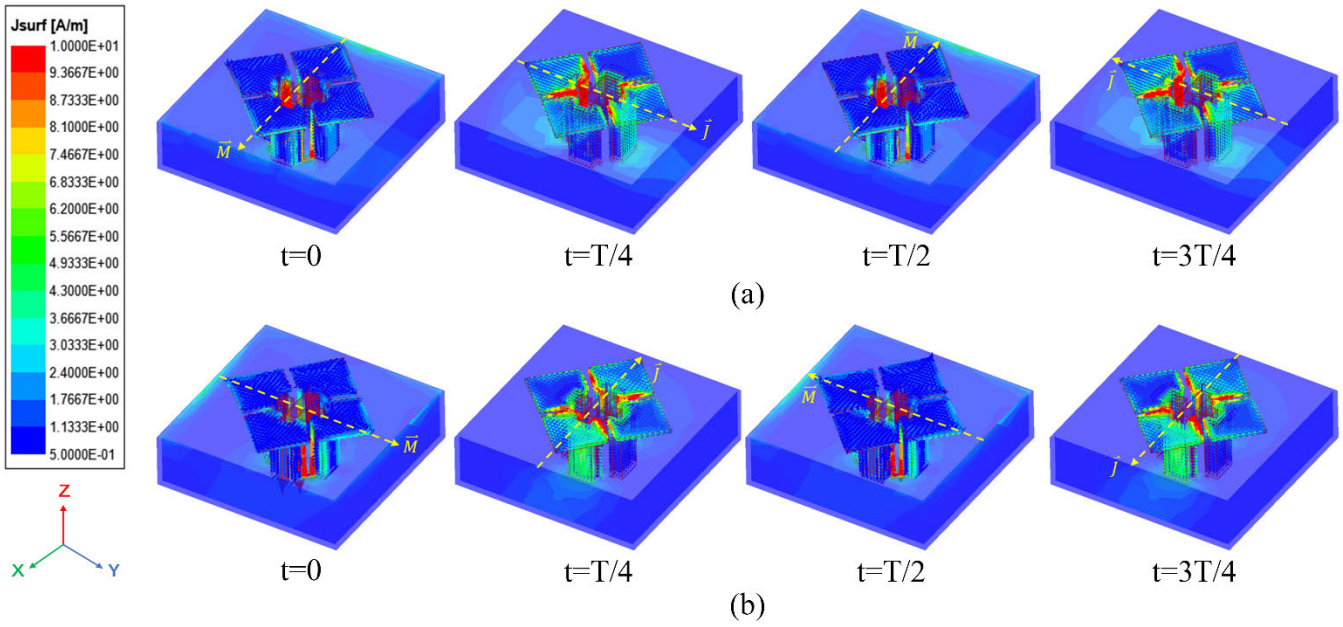

FIGURE 4. Current distribution of the proposed antenna at 3.3GHz. (a) Port1. (b) Port2.

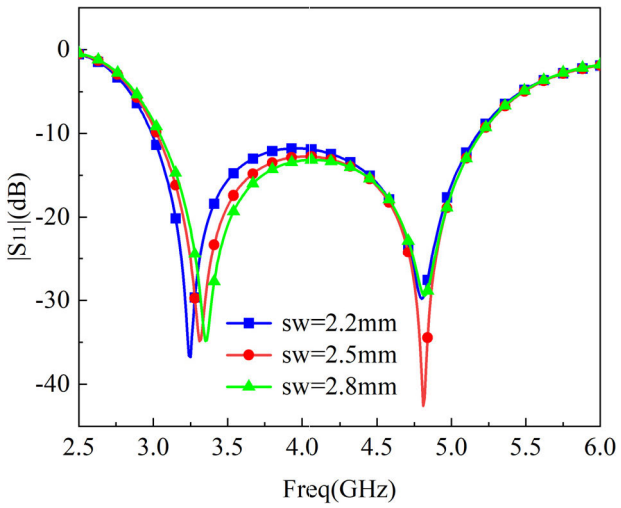

FIGURE 5. The influence of parameter sw on reflection coefficient.

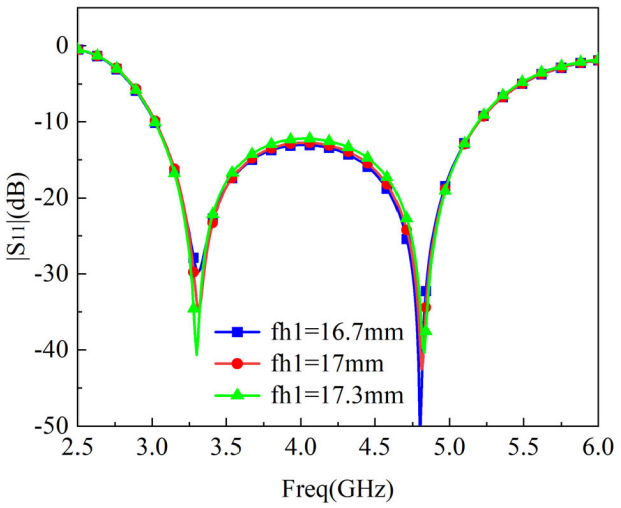

FIGURE 6. The influence of parameter fh1 on reflection coefficient.

shows a downward trend. In the optimization, it can be used to fine-tune the high frequency resonance.

C. EFFECT OF THE GW

The ground width GW has corresponding influence on the resonant frequency of the antenna. As shown in Figure 7, when the value of GW increases, the resonant point of low frequency moves to the right, while the resonant point of high frequency moves to the left, and the distance between the two resonant points becomes closer and closer, which reduces the working bandwidth range of the antenna. In addition, the impedance matching is improved obviously in the working frequency band.

D. EFFECT OF THE FW

Figure 8 depicts the variation curve of reflection coefficient with feeder width fw. It is observed that it has a great impact on the impedance matching of the whole frequency band. The larger the fw value, the worse the impedance characteristics. If the fw is larger than 3.8 mm, the overall antenna impedance will be mismatched. According to the simulation results, when the fw is 3.5 mm, the impedance matching is the best.

V. MEASUREMENT RESULTS AND DISCUSSION

To validate the performance of the proposed antenna, a prototype of the antenna is manufactured and the actual

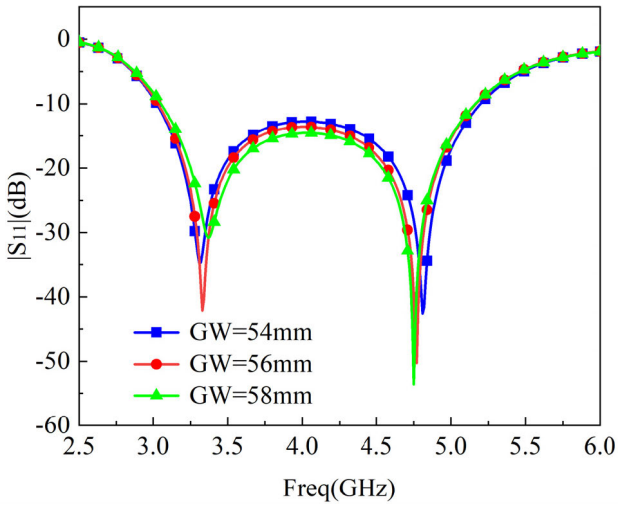

FIGURE 7. The influence of parameter GW on reflection coefficient.

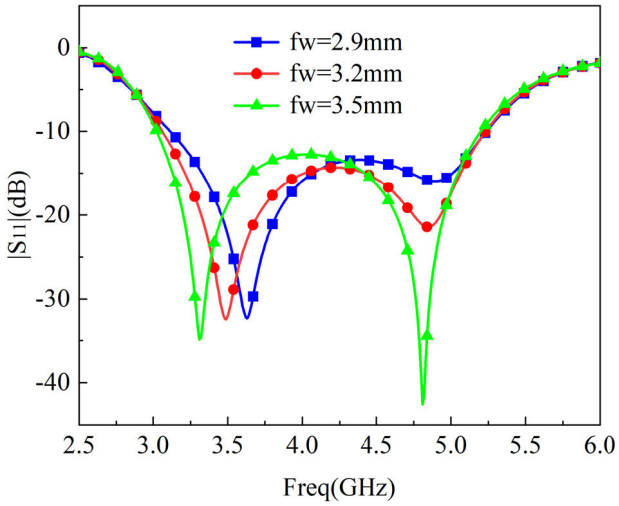

FIGURE 8. The influence of parameter fw on reflection coefficient.

FIGURE 9. Photographs of the fabricated antenna and measurement in the anechoic chamber.

measurements are carried out, the measurement results are elaborated in the following sections. Figure 9 shows the actual model and test scenario of the antenna.

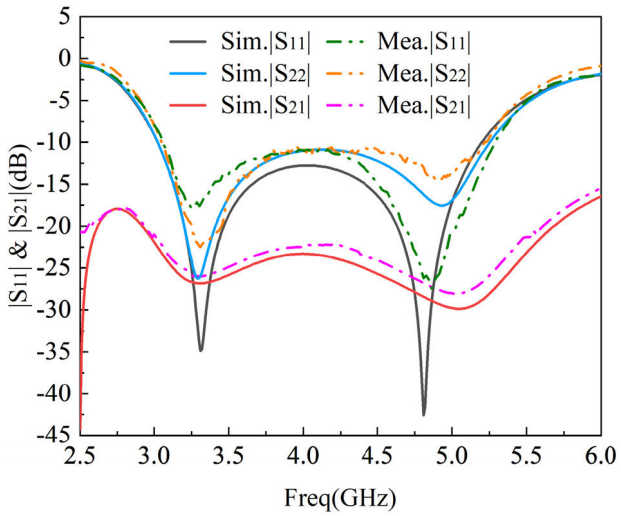

FIGURE 10. Comparison of simulation and experiment results of reflection coefficient and port isolation.

A. REFLECTION COEFFICIENT AND ISOLATION

The reflection coefficient and port isolation of the proposed antenna are measured by E5063A vector network analyzer. The simulation and measurement results are shown in Figure 10. The simulated and measured −10 dB impedance bandwidths are 53% (3.02-5.20 GHz) and 53.2% (3.06-5.28 GHz), respectively. The port isolation in the corresponding 5G operating frequency band is less than −22 dB. It is observed that there are some differences between the actual measurement results of the prototype and the simulation results, but the general trend is consistent, this is mainly caused by manufacturing tolerances and measurement errors.

B. GAIN AND RADIATION PATTERN

In the microwave anechoic chamber, the far-field radiation performance of the antenna is tested, and the gain curve and radiation pattern are obtained. The experimental results are shown in the following figure. The E and H planes of the proposed antenna show excellent symmetric radiation characteristics and stable radiation patterns at 3.3 GHz, 4 GHz and 4.8 GHz. The cross-polarization in the maximum radiation direction is less than −19 dB, and the cross-polarization in the range of ± 60° is less than −23 dB, which can meet the requirements of low cross-polarization required by the base station communication. In addition, in the operating frequency band, the proposed antenna has a high gain level, the peak gain can reach 9.6dBi, and the gain curve is relatively stable, the variation is only about 2.3 dB.

C. FRONT-TO-BACK RATIO AND BEAMWIDTH

In this section, the front-to-back ratio and half power beam width of the antenna are shown. Firstly, the influence of the back cavity structure composed of metal wall on the performance is studied. As shown in Figure 12, the electric field radiation of the proposed antenna in the far field is

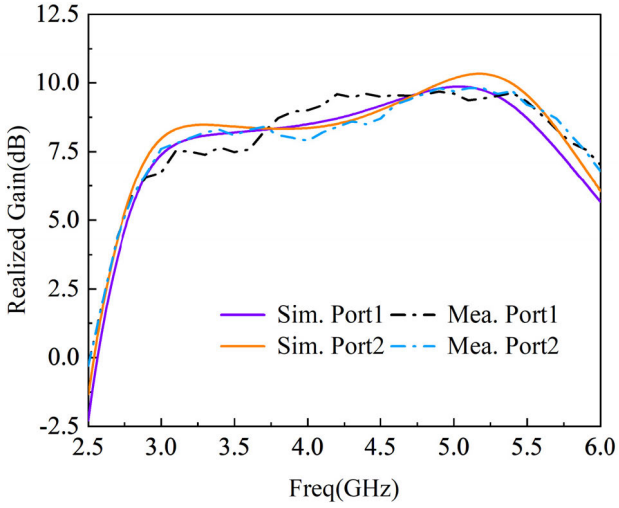

FIGURE 11. Simulation and measurement of realized gain curves of the proposed ME antenna.

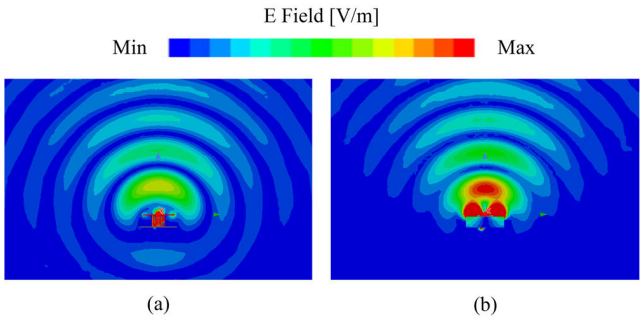

FIGURE 12. Far-field radiation of the proposed antenna. (a) Without metal wall. (b) With metal wall.

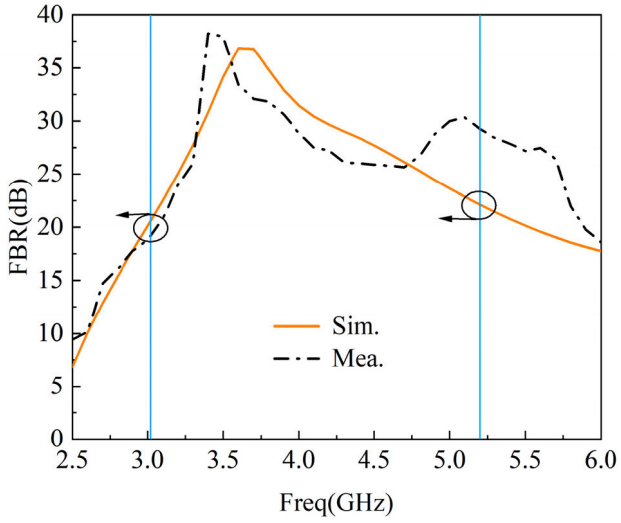

FIGURE 13. Comparison of the proposed antenna simulation and measurement front-to-back ratio.

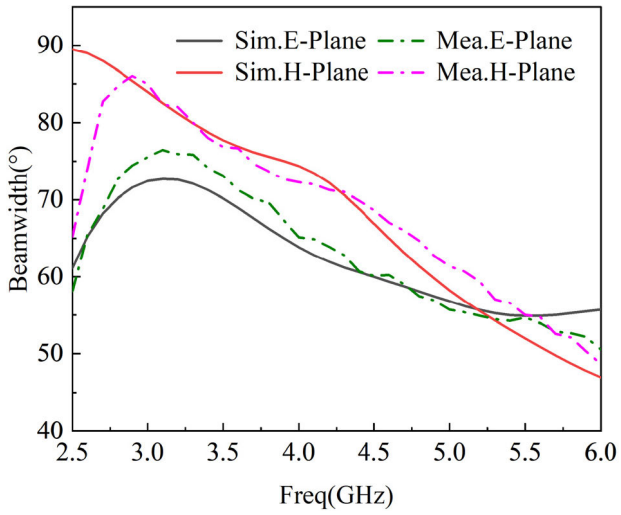

FIGURE 14. Simulation and measurement of the proposed antenna beamwidth in E-plane and H-plane.

simulated with and without a metal wall. From Figure 12(a), it can be clearly observed that the antenna exists backward radiation. Part of the electric field energy passes through the metal ground and covers a large wide-angle range. In contrast, in Figure 12(b), after the metal wall is loaded, the back radiation of the antenna is well suppressed, almost no electric field energy is transmitted, and the unidirectional radiation ability is enhanced. Through simulation analysis, the average gain of the proposed antenna is increased by 1.6dB.

In order to show the antenna's back lobe suppression level and beam coverage degree more intuitively. Figure 13 and Figure 14 plot the front-to-back ratio and the 3-dB beamwidth of the antenna as a function of frequency. It can be seen that in the whole impedance bandwidth range, the front-to-back ratio is greater than 20 dB, at about 3.7 GHz, the front-to-back ratio level is the highest, can reach 36 dB.

In addition, the 3-dB beamwidth of the antenna in plane E is between 55°-72°, and the beamwidth in plane H is between 55°-83°. The beam difference between the two planes at the same frequency is not more than 11°. In contrast, plane E and plane H have better symmetry. In conclusion, the proposed antenna has high front-to-back ratio and relatively stable beam coverage capability.

Finally, the performance of the proposed antenna is compared with some previous works. The details of the data indicators are shown in Table 2. Compared with the traditional ME antenna, the loading of the rectangular slot makes the feeder and the vertical patch form a coplanar structure, so that the transverse dimension (length × width) of the antenna is more compact. Although the size of the slack-coupled feed structure proposed in literature [23] is smaller, this design has wider bandwidth, higher front-to-back ratio and higher peak gain. In addition, references [16] and [17] have higher gain levels, but the work done by [16] is only single-linear polarization. In the design [17], the cross-polarization of the antenna at the two ports is only less than −8dB at the high frequency, which can be suppressed by adjusting the size of

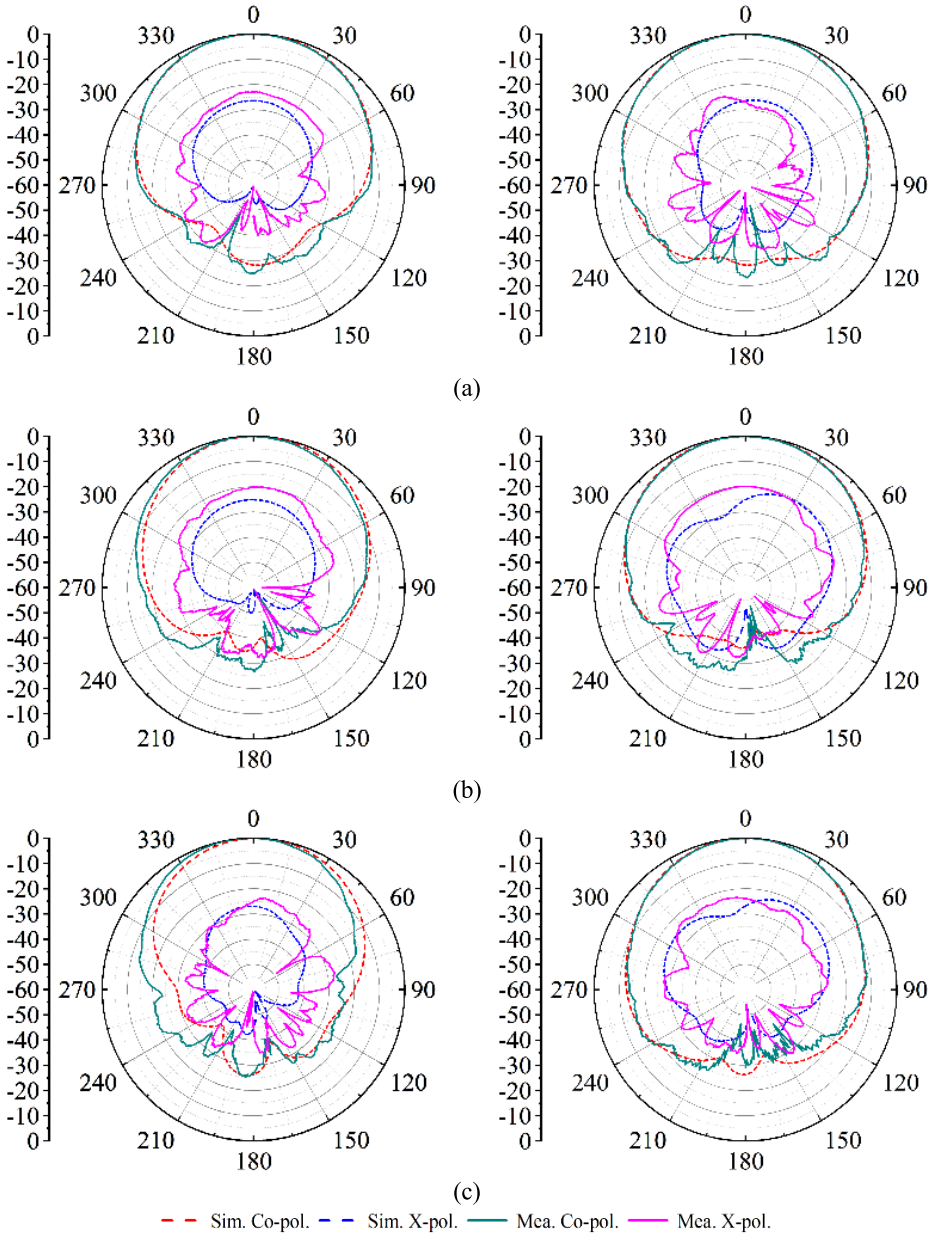

FIGURE 15. Simulation and measurement of the radiation pattern of the proposed antenna at port 1 excitation. (a) 3.3GHz. (b) 4GHz. (c) 4.8GHz.

TABLE 2. Comparison of this work with the previous designs.

Ref.	Transverse dimension (λ_{min})	Polarization	Relative bandwidth (%)	Peak gain (dBi)	Isolation (dB)	X-pol (dB)	Front-to-back ratio (dB)
[15]	0.79 × 0.81	Single-linear	41	6.7	/	< -20	> 15
[16]	0.94 × 1.06	Single-linear	46.2	10.19	/	< -35	Not mentioned
[17]	1.19 × 1.19	Dual-linear	55	10.8	< -35	< -8	> 20
[22]	0.74 × 0.74	Dual-linear	13.3	7	Not mentioned	< -15	About 20
[23]	0.50 × 0.50	Dual-linear	33	8.5	< -25	< -20	> 18
[24]	1.53 × 1.53	Dual-linear	36.7	9.36	< -17	< -15	> 20
Prop.	0.57 × 0.57	Dual-linear	53.2	9.6	< -22	< -19	> 20

the H-shaped ground, but the gain will be unstable. At the same time, the half-power beamwidth achieves about 48° ± 8° coverage in the whole band, which is not sufficient for base station communication applications. In comparison, the isolation degree and cross- polarization of this design is not the best, but the comprehensive performance is better. Meanwhile, the overall structure of the antenna is simple and low cost, which is conducive to manufacturing.

VI. CONCLUSION

A compact wideband dual-polarized magnetoelectric dipole antenna suitable for 5G base station is designed in this paper. The inverted L-shaped feeder is coplanar with the vertical patch, which can effectively excite the magnetoelectric complementary mode and contribute to the miniaturization of the transverse size of the antenna. The actual measurement shows that the -10dB impedance bandwidth of the antenna is 53.2% (3.06-5.28 GHz), and the full coverage of n77/78/79 band is realized. It exhibits stable high gain characteristics and symmetrical radiation patterns throughout the operating band. Meanwhile, the antenna has the advantages of simple structure, high ratio of front-to-back, better port isolation and cross- polarization recognition, which can well meet the needs of 5G base station communication.

REFERENCES

[1] D. Chandramouli, R. Liebhart, and J. Pirskanen, *5G for the Connected World*. Hoboken, NJ, USA: Wiley, 2019.

[2] M. Barba, "A high-isolation, wideband and dual-linear polarization patch antenna," *IEEE Trans. Antennas Propag.*, vol. 56, no. 5, pp. 1472–1476, May 2008.

[3] L.-H. Wen, S. Gao, Q. Luo, Q. Yang, W. Hu, and Y. Yin, "A low-cost differentially driven dual-polarized patch antenna by using open-loop resonators," *IEEE Trans. Antennas Propag.*, vol. 67, no. 4, pp. 2745–2750, Apr. 2019.

[4] J. Zhang, X. Q. Lin, L. Y. Nie, J. W. Yu, and Y. Fan, "Wideband dual-polarization patch antenna array with parallel strip line balun feeding," *IEEE Antennas Wireless Propag. Lett.*, vol. 15, pp. 1499–1501, 2016.

[5] Y.-X. Guo, K.-M. Luk, and K.-F. Lee, "Broadband dual polarization patch element for cellular-phone base stations," *IEEE Trans. Antennas Propag.*, vol. 50, no. 2, pp. 251–253, Feb. 2002.

[6] Y. Jin and Z. Du, "Broadband dual-polarized F-probe fed stacked patch antenna for base stations," *IEEE Antennas Wireless Propag. Lett.*, vol. 14, pp. 1121–1124, 2015.

[7] J. J. Chen, L. Li, H. Chen, Q. Fang, and X. L. Chen, "Design of miniaturized D-band dual-polarized dipole base station antenna based on coupling feeding," *Int. J. RF Microw. Comput.-Aided Eng.*, vol. 30, no. 4, Apr. 2020, Art. no. e22107.

[8] J. Hao, F. Wei, X. Zhao, and X. W. Shi, "A dual-polarized cross-dipole antenna with wide beam and high isolation for base station," *Int. J. RF Microw. Comput.-Aided Eng.*, vol. 30, no. 10, Oct. 2020, Art. no. e22373.

[9] L. Ye, G. Liu, Y. Li, J. Li, Z. Hu, and D. Wu, "Broadband dual-polarized crossed-dipole antenna with tapered integrated balun for base-station applications," *Int. J. RF Microw. Comput.-Aided Eng.*, vol. 31, no. 7, Jul. 2021, Art. no. e22687.

[10] G.-F. Cui, S.-G. Zhou, S.-X. Gong, and Y. Liu, "Design of a dual-polarized wideband antenna for 2G/3G/4G mobile communication base station application," *Microw. Opt. Technol. Lett.*, vol. 58, no. 6, pp. 1329–1332, Mar. 2016.

[11] H. Huang, Y. Liu, and S.-X. Gong, "An integrative dual-polarized antenna for broadband base station applications," *Microw. Opt. Technol. Lett.*, vol. 58, no. 12, pp. 2845–2851, Sep. 2016.

[12] J. Lee, H. Kwon, B. Kang, and K. Lee, "Design of a dual-polarised antenna with high isolation and a metallic cube for beyond 4G small base station applications," *IET Microw., Antennas Propag.*, vol. 8, no. 6, pp. 386–393, Apr. 2014.

[13] J. Zeng and K.-M. Luk, "A simple wideband magnetoelectric dipole antenna with a defected ground structure," *IEEE Antennas Wireless Propag. Lett.*, vol. 17, no. 8, pp. 1497–1500, Aug. 2018.

[14] K. He, S.-X. Gong, and F. Gao, "A wideband dual-band magneto-electric dipole antenna with improved feeding structure," *IEEE Antennas Wireless Propag. Lett.*, vol. 13, pp. 1729–1732, 2014.

[15] Y. Li and K.-M. Luk, "A linearly polarized magnetoelectric dipole with wide H-plane beamwidth," *IEEE Trans. Antennas Propag.*, vol. 62, no. 4, pp. 1830–1836, Apr. 2014.

[16] W. Liu, T. Wang, D. Gao, Y. Liu, and X. Zhang, "Low-profile broadband magnetoelectric dipole antenna with dual-complementary source," *IEEE Antennas Wireless Propag. Lett.*, vol. 19, no. 12, pp. 2447–2451, Dec. 2020.

[17] H. W. Lai, K. K. So, H. Wong, C. H. Chan, and K. M. Luk, "Magnetoelectric dipole antennas with dual open-ended slot excitation," *IEEE Trans. Antennas Propag.*, vol. 64, no. 8, pp. 3338–3346, Aug. 2016.

[18] X. Zhang, Y. Jiao, Z. Weng, Y. Zhang, and S. Feng, "Wideband magneto-electric dipole antenna with a claw shaped reflector for 5G communication systems," *Microw. Opt. Technol. Lett.*, vol. 61, no. 9, pp. 2098–2104, May 2019.

[19] J. Tao, Q. Feng, G. A. E. Vandenbosch, and V. Volskiy, "Director-loaded magneto-electric dipole antenna with wideband flat gain," *IEEE Trans. Antennas Propag.*, vol. 67, no. 11, pp. 6761–6769, Nov. 2019.

[20] L. Yang, Z. Weng, C. Zhang, and R. Du, "A dual-wideband dual-polarized directional magneto-electric dipole antenna," *Microw. Opt. Technol. Lett.*, vol. 59, no. 5, pp. 1128–1133, Mar. 2017.

[21] Z. Li, X. Chen, X. Hu, and D. Qiao, "A novel dual-linear polarized ultra-wideband magneto-electric dipole antenna with gain improvement," *Int. J. RF Microw. Comput.-Aided Eng.*, vol. 31, no. 12, Dec. 2021, Art. no. e22891.

[22] J. Y. Yin and L. Zhang, "Design of a dual-polarized magnetoelectric dipole antenna with gain improvement at low elevation angle for a base station," *IEEE Antennas Wireless Propag. Lett.*, vol. 19, no. 5, pp. 756–760, May 2020.

[23] C. H. Le Thi, S. X. Ta, X. Q. Nguyen, K. K. Nguyen, and C. Dao-Ngoc, "Design of compact broadband dual-polarized antenna for 5G applications," *Int. J. RF Microw. Comput.-Aided Eng.*, vol. 31, no. 5, May 2021, Art. no. e22615.

[24] J.-N. Sun, J.-L. Li, and L. Xia, "A dual-polarized magneto-electric dipole antenna for application to N77/N78 band," *IEEE Access*, vol. 7, pp. 161708–161715, 2019.

SHIHAO WU is currently pursuing the degree with the School of Science, Xi'an University of Posts and Telecommunications, Xi'an, China. His fields of expertise are electromagnetic fields and microwave technology. His research interests include broadband antennas and RF components.

FENG SHANG was born in 1966. He received the M.S. degree in electromagnetic field and microwave technology from Xidian University. He is currently a Professor with the Xi'an University of Posts and Telecommunications. His research interests include antenna theory and engineering, and RF signal process.